This invited presentation 2M-LS-O1.1 was given at EUCAS 2015. A manuscript was submitted to *IEEE Trans. Appl. Supercond.* for possible publication.

# Design and Testing of Real Scale $MgB_2$ Coils for SUPRAPOWER 10 MW Wind Generators

Gustavo Sarmiento, Santiago Sanz, Ainhoa Pujana, Jose María Merino, Iker Marino, Matteo Tropeano, Davide Nardelli and Gianni Grasso.

***Abstract*— Superconducting $MgB_2$ coils have a promising application niche in large wind generators. The potential implementation as field coils results in machines with smaller size and reduced weight, which is the real benefit compared to conventional non-superconducting alternatives. This is a key factor where wind market demands higher power rate and more compact turbines in order to optimize capital and operational costs.**

**Under the SUPRAPOWER project, a 10 MW direct drive wind generator concept will be probed through an experimental scale validator, where superconductivity is implemented in the rotor DC coils. For the required operational temperature, current density and magnetic field the available commercial $MgB_2$ wire has been selected, as it is a cost effective and well suited compared to other solutions.**

**The aim of the present work is to analyse the operational conditions of MgB2 DC field coils, cooled by a cryogen-free system and developed according the required performance for the SUPRAPOWER generator. The paper deals with the design, manufacturing and experimental results of such full scale superconducting coils.**

***Index Terms*— cryogen-free, MgB2 coil, superconducting generator, wind turbine**

## I. Introduction

OFSSHORE WIND sector is a growing market, being the global cumulative install capacity at end of 2014 8,759 GW, with 88% installed in Europe [1]. Economic reasons focus to the installation of higher power density ratio turbines. In fact, average rated power of new installed turbines is expected to reach 6 MW in 2016 and 8 MW in 2020 [2]. However, more powerful turbines mean larger generators, especially in direct drive (DD) trains.
Superconducting windings permit to achieve strong magnetic fields because of their capability to carry high current densities. That has been the base to develop more compact power machines, i. e. lighter than using conventional resistive technology.

Superconducting generators for wind turbines has the potential to reduce drastically the weight and volume, fundamentally in DD machines. Nowadays, several wind generator concepts are under different development stagest [3-7]. All of them focused in 10 MW power machines or higher. Attending just superconducting issues, there are several aspects to underline in the generator design: superconductor and cooling system selection and machine topology. Extensive reviews and studies have been done regarding the use of High Temperature Superconductors (HTS) [8, 9] and different machine topologies [10]. $MgB_2$ wire has focused designers attention due to its good performance-cost ratio at relatively high operation temperatures; around 20 K [6, 11, 12]. The implementation in wind generators of such material requires the experimental validation of coils [13].

In this paper the design of DC field coils for the SUPRAPOWER 10 MW DD generator [14] is presented. They consist in a stack of nine doubles pancakes (DP), specifically designed to be cooled under cryogen free conditions. Experimental results of one prototype DP are discussed.

## II. Description of the $MgB_2$ Coil

### A. $MgB_2$ Coil Design

SUPRAPOWER 10 MW wind generator concept is a partially superconducting machine with warm iron poles [11, 14]. Superconducting coils are the generator induction field coils while copper (Cu) is used for the AC armature winding. Field coils are enclosed individually in modular cryostats [15] to ensure cryogenic conditions. Conduction cooled system based in a cryogen-free ones has been considered as the most suitable for offshore wind SUPRAPOWER concept. Therefore each coil is thermally link to a thermal collector that sinks the heat into GM cryocoolers.

The field coil CAD model is presented in Fig. 1. Coils are a stack of nine serial connected $MgB_2$ double pancake (DP) racetrack coils, sandwiched between two copper plates. Those plates mechanically fix the assembly and are a fundamental part of the thermal circuit to refrigerate each DP. Coil straight parts are mechanically reinforced with wedges and counter-wedges. Threaded rods fix the Cu plates tightening with plates reinforcements.

DPs are the basic elements of the coils. They are constituted by two $MgB_2$ wire layers with a Cu sheet in between. Each DP is thermally connected to the Cu plates through massive Cu parts so-called combs, which are connectsed to the laps that arise from each internal Cu sheet. Therefore, a homogeneous refrigeration of each $MgB_2$ wire turn is guaranteed. $MgB_2$ wire has been selected among others superconductors, attending its performance-cost ratio. For the selected machine architecture

The research leading to these results has received funding from the European Union Seventh Framework Programe (FP7/2007-2013) under SUPRAPOWER project, grant agreement n° 308793.

G.Sarmiento, S. Sanz, A. Pujana, J.M. Merino and I. Marino are with TECNALIA. Parque Tecnológico, Edificio 700. 48160 Derio, Spain (e-mail: gustavo.sarmiento@tecnalia.com).

M. Tropeano, D. Nardelli and G. Grasso are with Columbus Superconductors SpA. Via delle Terre Rosse, 30 16133 Genova Italy.

is very suitable according to the peak field, below 2 T.

As a first step a DP prototype, called SC4, has been built (see next paragraph). The aim is twofold: In one hand to define and validate a manufacturing procedure. On the other hand, to validate the mechanical, thermal and electromagnetic design by means of the DP experimental test. In this sense, some previous experiences with a 7 turns solenoid called SC2 [16] and a 30 turns solenoid SC3 have been realized. SC3 was built to validate the winding, impregnation and test procedures to be applied in SC4.

$MgB_2$ wire is provided by Columbus SpA, and is presented in form of sandwich tape, with a soldered outer copper stabilization strip in one tape side. $MgB_2$ powder is ex-situ reacted, then sintered in the wire, Cu strip soldered and insulated before winding. Table I summarizes the main features of the Batch V1579, used in the SC4 coil manufacturing. $I$-$\mu_0 H$ characteristics are shown in Fig. 2.

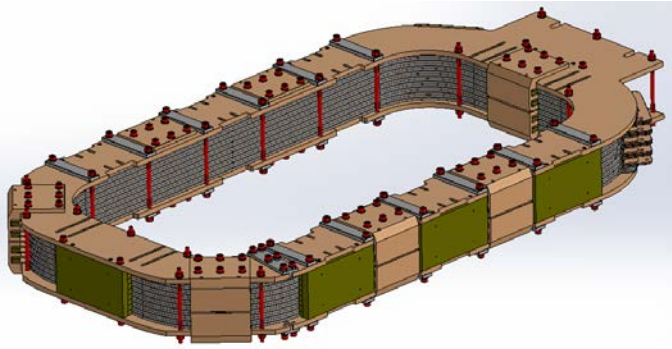

Fig. 1. 10 MW generator field coil CAD model. Note it is a stack of nine double pancakes, prepared to be refrigerated under cryogen-free conditions.

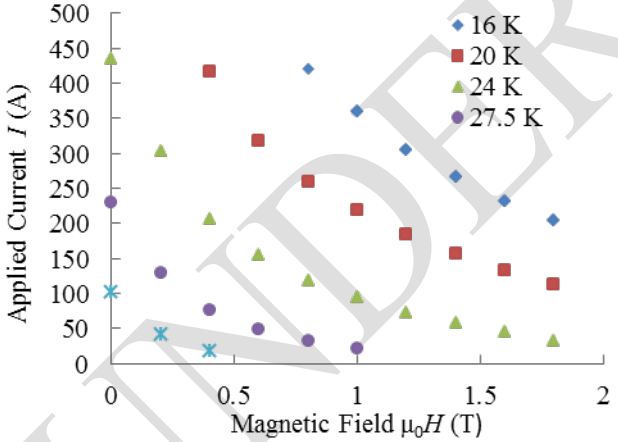


Fig. 2. Wire performance for batch V1579

Combining wire parameters with coil and generator joint electromagnetic design the operation conditions at 20 K are defined: charge load current of 95 A, and 1.37 T coil peak field. The calculations show that the field circuit inductance is, including iron poles, 9.27 H.

### *B. SC4. Double Pancake Coil Specifications*

SC4 is made of two identical layers wound in opposite direction, continuously, without splices. As mentioned before, a 2 mm Cu sheet is located in between for refrigeration purposes; it is enameled in order to provide additional insulation to the wire layers. Winding process was made in CIEMAT facilities. Once finishing the winding, the DP was vacuum impregnated with Araldit F resin and cured at TECNALIA facilities. Table I summarizes the main design parameters for SC4. Fig. 3 shows the result, achieved after the third attempt. The main difficulty is to handle the wire as it is a soft structure made of a Ni sheath with an annealed Cu strip (Table I). Minimum bending diameter is set in 150 mm for practical purposes according manufacturer, recommending leaving Cu strip in the outer part of each winding turn [17]. In the SC4 development, it is set to 200 mm.

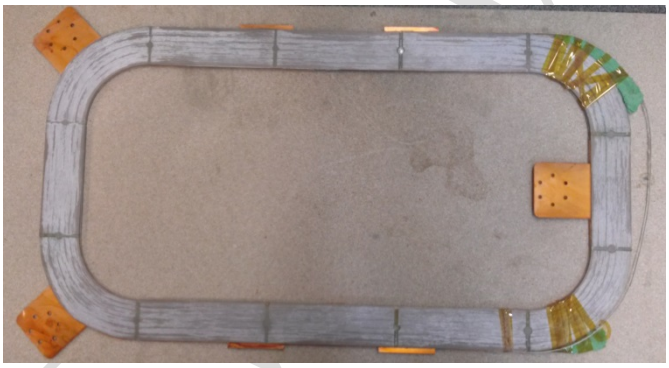

Fig. 3. Picture of the SC4 DP experimental realization.

## III. EXPERIMENTAL DETAILS

SC4 has been tested in a cryogen-free cryostat in the TECNALIA Applied Superconductivity Laboratory. Cooling is done by means of a two stages Gifford-McMahon (GM) cryocooler (COOLPOWER 10 MD cold head and COOLPAK 6000 MD helium compressor, by Oerlikon-Leybold Vacuum). Four current leads can be used to energize coils, permitting a maximum DC current injection of 300 A per pair. 1st stage is connected to the radiation shield- an aluminum case plus MLI blankets- to keep it below 100 K. Current leads first part (from 300 to 80 K) is made of DHP Cu tubes thermally anchored to a heat sink connected to the 1st stage at around 80 K. Its second part (from 80 to 20 K) is made of four Sumitomo 1G-(DI-BSCCO) Type HT tapes in parallel per pole, encased into a PE tube, which become rigid at low temperatures.

SC4 is refrigerated by physical connection of the cryocooler 2nd stage to the Cu sheet in order to ensure a thermal homogeneity, as every turn is in direct contact to this cooper layer. The thermal connection is achieved by means of OFE Cu braids, which are screwed to laps using Apiezon® type N cryogenic grease to enhance thermal conductivity.

Fig. 4 shows the assembly of the Cu braids; three of them were used to refrigerate the Cu sheet –screwed to the laps-. Other two were used to keep cold the electric joints. The coil wire terminals were not encapsulated together with the rest of the coil during the impregnation process, but they were left free. Cu massive parts were soldered afterwards (Fig. 4). A G11 glass fiber support was made in order to hold the copper part in position and thus to avoid wire terminal damage. They are large enough to screw directly a copper braid. Note that same copper part was used to feed electrically the coil and also to refrigerate the electrical joint. HTS leads are connected by

pressure and Indium foil interfaces to the electrical exit to feed the DP. Note that the Cu braids are insulated with a 0.2 mm G11 layer.

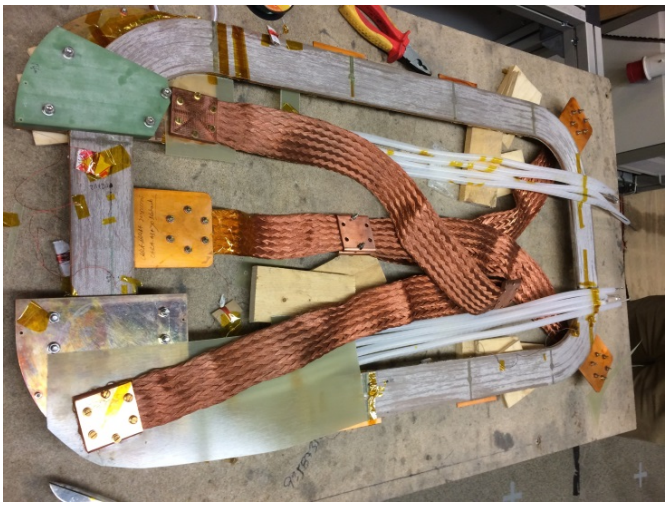

Fig. 4. Setup of the SC4, including copper braids

Both SC4 winding layers and the layer jump were monitored. Fig. 5 shows the sketch of voltage taps distribution, each labeled with and initial "v" and inside a round globe. The voltage taps were performed by milling carefully the coil surface, removing the epoxy and the Dacron® insulation. Voltage taps consist on Ø0.2 mm enameled copper wires. Then the soldering point is protected with Stycast® epoxy resin. Each voltage tap pair is twisted and braided as near as possible to the soldering points, in order to prevent electromagnetic noise. A magnetic Hall sensor is positioned (see Fig. 5) near to the coil peak magnetic field in the inner side of the curved parts. It measures the field perpendicular to the coil plane. Magnetic field measurement is important as it is a direct indication of the current passing across the coil; it is also needed during data treatment to remove the inductive voltage.

During the coil winding the wire was accidentally bent beyond the maximum bending radius in two different segments. These zones were monitored with voltage taps in order to examine their behavior (lengths located between V27V2-V27V1 & V60V2-V60V1). Last, a heater was installed to start artificially a quench. Some voltage taps have been installed around to investigate the quench propagation in future studies.

Several thermometers have been located around the setup: Cernox®, Pt100, silicon diodes, and a calibrated CCS (Carbon Ceramic Sensor) lend by the manufacturer Temati. Location is shown in Fig. 5, circled inside a hexagonal globe., some of them, located in the refrigeration laps. CX3 has been set close to the quench resistor (in the inner part of the coil) and CX4 on the Cu insert. Besides SC4, also the copper electrical exits were monitored, as well as the HTS tapes warm side (not shown in the sketch).

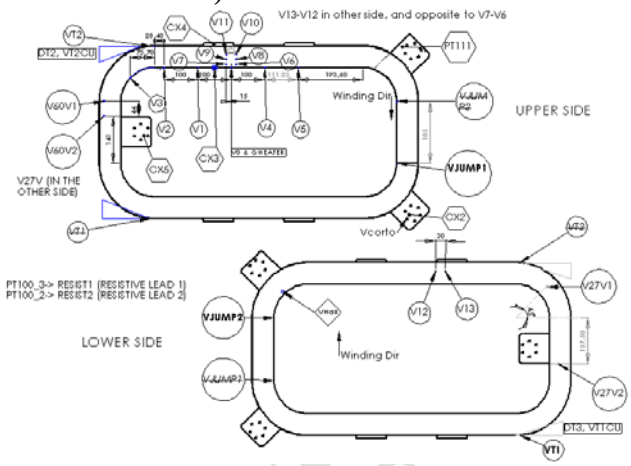


Fig. 5. Distribution of the Voltage taps and thermometers

Fig. 6 shows the SC4 hanged with Nylon® wires from a glass fiber frame (G11), specifically design to stand the coil and braids weight minimizing the heat load by conduction through supports from the radiation shield. Therefore, the coil is tested suspended from the G11 frame. Fig. 6 (left) shows the lifting process through the frame. In Fig. 6 (right) the SC4 and the frame together are shown inside the cryostat.

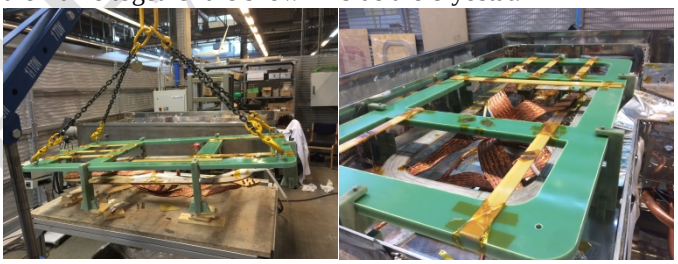

Fig. 6. SC4 set up prior test. Left: lifting process of the SC4 and the frame. Right: SC4 in the cryostat before to be tested.

## IV. Results and Discussion

Fig. 7 presents the load lines for selected segments in the coil. Calculated load lines and wire critical current have been plotted in a *I-B* diagram. It is worth to point out that the ferromagnetic Ni component of the wire influences the magnetic field following the expression $B = \mu_0(H + M)$. In order to compare fairly, the *I-B*(T) characteristic must be used to account the Ni behavior. Therefore, pure Ni magnetization has been added to the magnetic characteristics of the wire showed in. Fig. 2; pondered by its volume fraction. It is assumed that the ferromagnetic Ni sheath behaves as pure Ni and simulations have been done considering a homogenous magnetic material distribution in the wire, neglecting the true wire architecture [16]. Load lines are not straight due to ferromagnetic material.

*I-B* characteristics are very useful to correctly interpret the magnetic sensor measurements located in the experimental setup or over the coil. Indeed Hall effect based sensors measure magnetic flux density *B* (T).

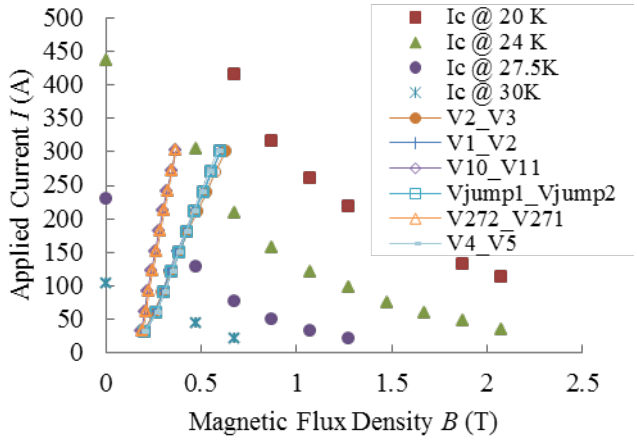


Fig. 7. Load lines of SC4 selected segments vs wire performance. Ni behavior has been taken into account.

Fig. 7 also shows the different performances of each segment. Magnetic field is different in each turn, thus a family of load lines is obtained.

Superconducting transitions at reduced current (around 0.5 – 1 A) were achieved in fixed intervals for each monitored segment. When the $MgB_2$ reaches its critical temperature, the voltage drops sharply. Transition temperature in the superconductor has been estimated through the analysis of the curves shown in Fig. 8, and the temperature registered in thermometers situated through the copper insert laps. The estimated temperature for the transition is 35.7±0.4 K During cooling down, due to the low power heat extraction, the transitions happen in long periods. It is clear that temperature gradients exist between different wire segments in the coil. In fact, turns closer to the Cu refrigerating laps are the first to transit, as expected: Ev2_v3 and Evjump1_vjump2. Afterwards, the transition is observed in the nearby segments and then in the rest ones. The coil temperature stabilization achieved through the copper sheet is clear. Evt1_vt2 represents the whole coil electric field being an average coil behavior. Once the whole coil has become superconducting, the cooling system is stopped. Therefore, temperature rises slowly and transitions happen again -Fig. 9- . However the DP is more isothermal, as it is indicated by the grouped curves.

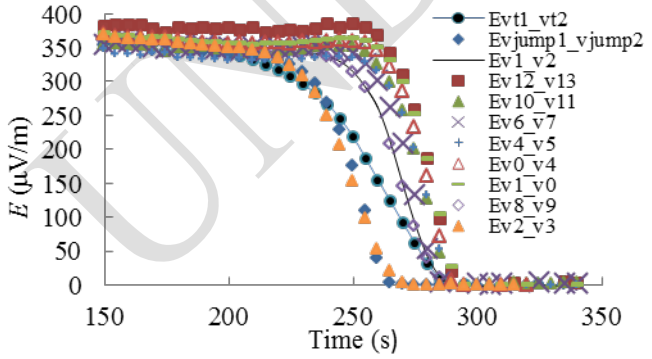


Fig. 8. Transitions with $I_{bias}$ of 0.9 A during cooling down.

Fig. 10 shows how magnetic simulations match fairly the experimental data. Presented measured magnetic flux density *B*(T) is done with the Hall sensor at 24 K, and same performance is found for other temperatures. Current is measured with a shunt resistance in series with the current supply. *B*(T) is increased monotonically with current, but it is not a perfect straight line. On the contrary, the magnetic field should be a straight line if there were not Ni or other magnetic materials in the wire, and the obtained magnetic flux density should be lower. Simulations including Ni in wire (following the aforementioned approximations) reproduce better the coil performance. The agreement between the measured and the (Ni) simulated values in the measurement point also evidences that all the turns are collaborating to generate the magnetic field; i. e. there are not short-circuited turns.

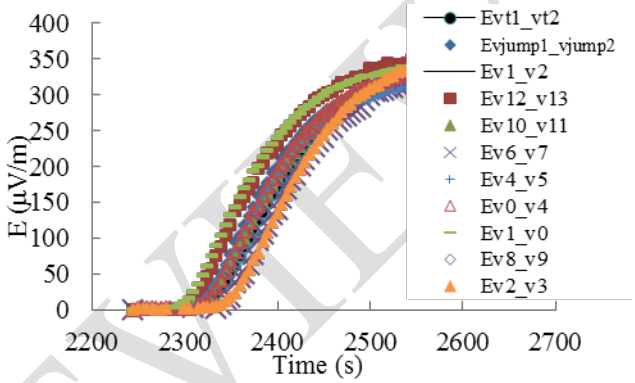


Fig. 9. Transitions with $I_{bias}$ of 0.9 A during heating up the system by switching off the cryocooler.

Fig. 11, up, shows an example at 30 K of the way in which the current is applied. It is done in steps, as smooth as possible in order to avoid the inductive voltage effects. However, Fig. 11, bottom, shows how inductive peaks appear due to current injection steps. Data is filtered in order to eliminate the inductive voltage from the *E* (V/m) vs *I* (A) characteristics, based in the recorded *B* (T). Selected voltage taps performance are presented, whose locations can be found in Fig. 5. Note the time scale in which the quench transition appeared for each voltage taps.

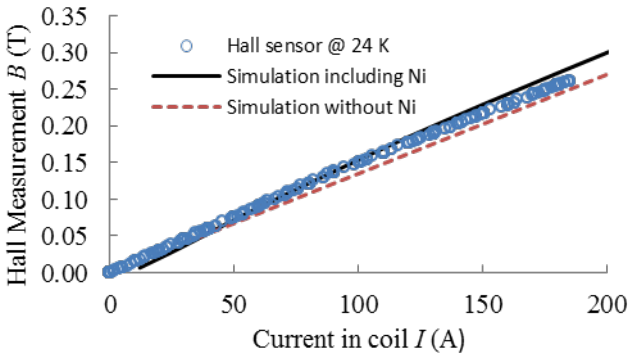


Fig. 10. Simulated expected current in Hall sensor vs true measurement

SC4 were tested at several temperatures. Despite the operation temperature for the superconducting wind generator will be around 20 K, the applied current limitation of 200 A (due to the HTS current leads setup particular limitation) prevented to go down in the temperature test. Therefore the obtained data make sense only for T > 27 K.

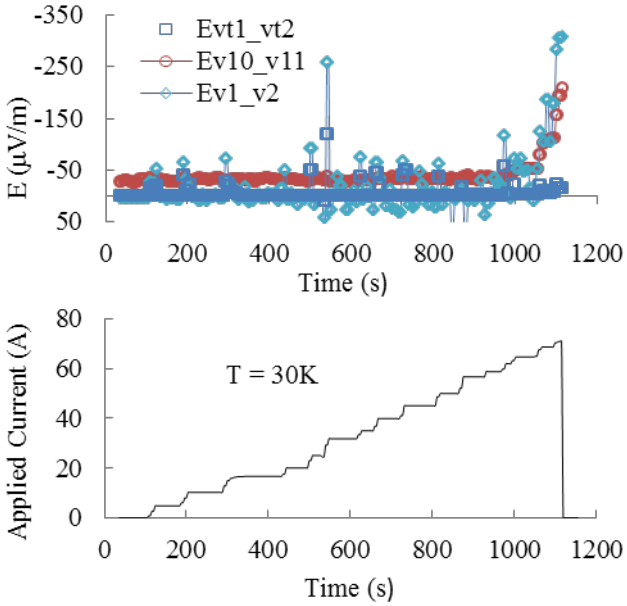


Fig. 11. Up: Evolution of the electric field *E* (V/m). Bottom: Current applied vs time

SC4 thermal behavior during current injection at 30 K is shown in Fig. 12. Thermometers locations are presented in Fig. 5. Silicon diode thermometers Dt2 and Dt3 are located in the current injection zones; their evolution indicates the goodness of the coil current transfer. Dt3 indicates that the corresponding terminal presents a higher electrical resistance (higher heat generation) comparing to Dt2 monitored joint.

Regarding the rest of thermometers and despite the shift (due to different contact resistance and not to substantial temperature gradients as proofed by the resistive to superconducting transitions), the evolution presents the same soft trend. In fact, the temperature increase for each sensor is less than one tenth of degree during the current injection. For example, CX2 is located (see Fig. 5) on one lap, almost opposite the location of CX4 (directly on the Cu insert): the recorded temperature for both sensors is virtually the same. Therefore, despite the cryogen-free conduction cooling system and the cryostat limitations to keep fixed the temperature during the current injection, the overall behavior indicates that the system temperature is stable during experiment.

Finally, the elbow (Fig. 12) showed in all the curves, is explained by the copper insert heating when the current supply is suddenly switch off. Such as abrupt event induces eddy currents in the conductive parts, and especially in the copper ones.

*E-I* characteristics have been obtained at 27 K, 28.5 K and 30 K. Filtered curves are adjusted with a potential function, $E=E_0\ (I/I_c)^n$. where E is the voltage developed per unit of length or electric field, $E_0$ is the criterion (usually $10^{-4}$ or $10^{-5}$ V/m). The adjusting parameters are the critical current $I_c$ and the n-value. It is important to note that obtained $I_c$ is not in perfect isothermal conditions, but the current is increased waiting only few seconds to reach voltage, but, in principle, not to a complete thermal stabilization. Table II summarizes the main analyzed segments, jointly to the whole superconducting coil (Evt1_vt2). The rest ones have been not shown either because they are not transited (that is the case of V27V2-V27V1 and V60V2-V60V1, the potentially damaged segments) or simply they had not enough resolution to be fitted.

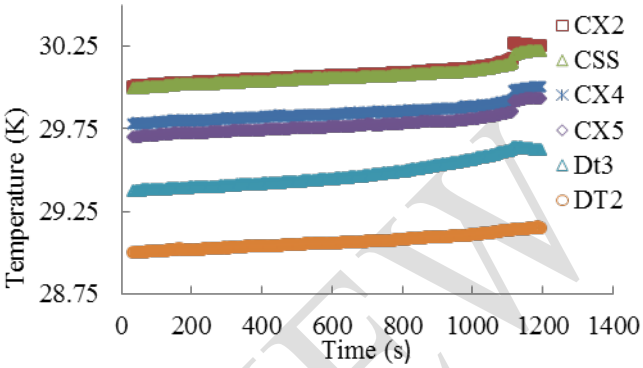


Fig. 12. Thermometers evolution during the V vs I test at around 30 K. Note the elbow due to heat generated by the eddy currents

Segments critical current differences are explained by two reasons:

- The first one is because not all the coil turns/segments are under the same magnetic field. This fact has been indicated in the calculated load lines for each segment, shown in Fig. 7.
- The second one is because, when close to the quench event, the thermal dissipation begins to be significant in the turns (and monitored segments), which slightly lower the estimated critical current. Cooling down in cryogen-free conditions is not immediate compared to cryogens bath. In addition, data acquisition system (DAQ) has a finite time delay (channels are sequentially acquired in the DAQ and not simultaneously, an inherent drawback of our existing Laboratory). That means that the recorded data in the segments belongs to past times, but during the analysis they are fit as "present" time. Therefore, there is also a systematic error in the values determination for these segments.

Fig. 13 shows the $I_c$ vs. temperature fitting. Despite the considerations taken before, regarding the critical currents obtained for the segments, the evolution presents a similar trend that for the $I_c$ for overall coil. The n-value should be only considered valid for the overall coil (Evt1_vt2), with a value around 10 at the studied temperatures. Measurements made in short samples of the same batch provided by Columbus SpA., and fitted at 20 K and 27.5 K shown n-values of 24 and 25.6 respectively. The origin of this overall reduced n-value is still not well understood. Note that the obtained critical currents in the selected segments are consistent with expected results derived from the calculated load lines in Fig. 7.

It would be also interesting to measure the quench propagation velocity by inducing an artificial quench in a given position with a heater. As it is needed a DAQ time resolution short enough, those measurements will be extensively done in further experiments, as a heater has already been implemented to be compared with the quench simulations.

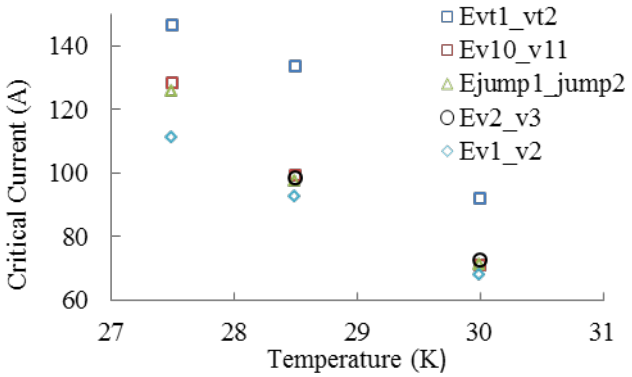


Fig. 13. Fit results: Critical current versus temperature.

## V. Conclusion

The design of the field coils of a 10 MW superconducting generator is presented. The coil is a stack of nine racetrack-type double pancakes, assembled to be cooled under restricted cryogen-free refrigeration. $MgB_2$ in tape form and stabilized by a Cu strip has been selected among others superconductors based in the good performance-cost ratio and operation temperature.

Prior to manufacture the field coil, a DP prototype, named SC4, was built to probe the manufacturing process and the design by testing under cryogen-free conditions.

The refrigeration strategy has been to cool down directly each turn of the coil. This design objective has been achieved by placing an OFE Cu sheet between the two DP winding layers and it has been shown very effective, showing a homogeneous temperature distribution. During current injection, temperature variation is less than one tenth of degree up to the quench trigger. Magnetic flux density generated in a selected SC4 area were measured. Obtained data agrees well with the simulations including Ni sheath magnetization. The ferromagnetic behavior of wire components has to be taken into account in the coils design and in the comparison with the experimental data.

Critical current at 27 K, 28.5 K, and 30 K were obtained in selected coil segments. Values are consistent with the load line calculations. Global coil n-value is around 10, lower than the expected, according to the batch short samples measurements.

Further quench studies are required. In summary, SC4 realization and its test results confirm the design and manufacturing process to keep developing the 10 MW superconducting generator field coils. Such a coils would possibly be useful in other application, e.g., fault current limiters.

## Acknowledgment

Authors would like to thank Luis Garcia-Tabarés, head of the Electrical Engineering Unit of CIEMAT, José Luis Gutiérrez Ruiz, and Daniel Lopez Rodríguez, form CIEMAT, for their assistance during the SC4 coils manufacturing process.

TABLE I
MgB2 Field Coils Specifications

| Coil | Stack of racetrack DPs |
|---|---|
| Number of DPs | 9 |
| Number of copper caps | 2 |
| Thickness of copper cap | 8 mm |
| Insulation layers between DPs | G11 |
| Insulation layer thickness | 0.2 mm |
| Total thickness stack | ~77.6 mm |
| Coil radius (curved parts coil ends) inner/outer | 100 mm / 165 mm |
| Total thickness | ~93.6 mm |
| Straight side length end parts | 185 |
| Straight side body | 622 |
| Total Wire length | ~ 3200 m |
| **SC4** | **Racetrack DP coil** |
| Mean dimension per wire in the coil | 3.200 x 0.885 mm |
| Number of turns per layer | 72.5 |
| Number of layers | 2 |
| Layer jump length | 185mm |
| Total number of turns | 145 |
| Cross section | 65.4 x 8.40 mm2 |
| Number of Copper sheet | 1 |
| Copper sheet thickness | 2 mm |
| Total thickness coil | 8.40 mm |
| Inner / outer coil radius | 100 mm / 165.4 mm |
| Straight side length end parts | 185 mm |
| Straight side active parts | 622 mm |
| Total wire length | ~356 m |
| Impregnation | Araldit F, (VPI) |
| Minimum Ic,coil @ 20 K | 355 A |
| Maximum Bc,coil @ 20 K | 0.78 T |
| Self-induction | 56 mH |
| Resistance (T=300 K) | 6.61 Ω |
| **MgB2 wire** | **Sandwich class** |
| Batch | V1579 |
| Sheath | Ni |
| Dimensions | 3 x 0.5 mm |
| Number of $MgB_2$ filaments | 19 |
| Filling Factor (no stabilizer) | 24.1% |
| Stabilizer | Cu strip (RRR 150) |
| Stabilizer features | One side, 0.2 mm, SnPb soldered |
| Insulation | Dacron 62.5 μm |
| Wire dimensions (bare) | 3 x 0.7 mm |
| Wire dimensions (insulated) | 3.125 x 0.825 mm |
| $I_c$ @ $\mu_0 H$= 1.8 T, 20 K | 113 A |
| dIc/dB @ $\mu_0 H$=1.8 T, 20 K | 100 A/T |
| Jce,wire (A/mm2) @ $\mu_0 H$= 1.8 T, 20 K | 58.18 A/mm2 |
| Bending diameter (practical, Cu layer outside) | 150 mm |

## References

TABLE II
Critical Current fit in selected SC4 segments. $I_c$(A), $E_0$($10^{-4}$ V/m)

| T (K) | Ev1_v2 | Ev2_v3 | Ejump1_jump2 | Ev10_v11 | Evt1_vt2 |
|---|---|---|---|---|---|
| 30 | 68.15 | 72.45 | 71.43 | 70.69 | 91.79 |
| 28.5s | 92.58 | 98.51 | 97.68 | 99.33 | 133.59 |
| 27.5 | 111.16 | | 125.96 | 128.12 | 146.26 |

[1] Global Wind Energy Council Report 2014 Annual Market Update 2014
[2] Roland Berger Strategic Consultants Report 2013 "*Offshore wind toward 2020 - On the pathway to cost competitiveness*"
[3] R. Fair et al "*Next Generation Drive Train -Superconductivity for Large-Scale Wind Turbines*" Presentation in Applied Superconductivity Conference 2012 (Portland, Oregon)

[4] AMSC SeaTitan 10 MW HTS Direct Drive Wind turbine, available at www.amsc.com.
[5] A. B. Abrahamsen, N. Magnusson, B. B. Jensen and M. Rundeb "*Large superconducting wind turbine generators*" Energy Procedia 24 60-67 2012
[6] P. J. Masson "*Wind turbine generators: Beyond the 10 MW frontier Presentation at Symposium on Superconducting Devices for Wind Energy systems*" 2011 (Barcelona)
[7] J Wang, R. Qu, Y. Tang, Y. Liu, B. Zhang, J. He, Z. Zhu, H. Fang, and L. Su. "*Design of a Superconducting Synchronous Generator with LTS Field Windings for 12 MW Offshore Direct-Drive Wind Turbines*" IEEE Transactions on Industrial Electronics. vol.PP, nº 99, pp.1-1
[8] B. B. Jensen, N. Mijatovic, and A. B. Abrahamsen, "*Development of superconducting wind turbine generators*" J. Renew. Sustain. Energy, vol. 5, no. 2, p. 023137, Mar. 2013.
[9] J. Lloberas, A. Sumper, M. Sanmarti, X. Granados "A review of high temperature superconductors for offshore wind power synchronous generators" Ren. And Sust. Energy Rev. 38 404-414 2014
[10] R. Qu, Y. Liu and J. Wang "*Review of Superconducting Generator Topologies for Direct-Drive Wind Turbines*" IEEE Transactions on Applied Superconductivity 23 5201108 2013
[11] A. Pujana, I. Marino, G. Sarmiento, S. Sanz, J. M. Merino and J. L.Villate "*Application of $MgB_2$ in Superconducting Wind Turbine*" Generators Proc. EWEA Wind Energy Event 2014 (Barcelona)
[12] S. Kalsi "Superconducting Wind Turbine Generator Employing MgB2 Windings Both on Rotor and Stator". Kalsi. IEEE Transactions on Applied Superconductivity, vol. 24, no. 1, February 2014
[13] A.B. Abrahamsen, N. Magnusson, B. B. Jensen BB, D Liu and H. Polinder "*Design of an $MgB_2$ race track coil for a wind generator pole demonstration*" J. Phys.: Conf. Ser. 507 032001 2014
[14] M. Scuotto, G. Sarmiento, J. M. Merino Azcárraga, J. García-Tejedor, P . Ibañez, S. Apiñániz Patent Application WO2011080357 A1, PCT/ES2009/070639 2009
[15] J. Sun, S. Sanz. H. and Neumann "*Conceptual design and thermal analysis of a modular cryostat for one single coil of a 10 MW offshore superconducting wind turbine*" CEC/ICMC 2015 (Tucson, Arizona) 2015
[16] G. Sarmiento, S. Sanz S, A. Pujana, J. M. Merino, R. Iturbe, S. Apiñaniz, D. Nardelli and I. Marino "*Design, manufacturing and tests of first cryogen-free MgB2 prototype coils for offshore wind generators*" J. Phys.: Conf. Ser. 507 032041 2014
[17] P. Kovac, L. Kopera, T. Melisek, G. Sarmiento, S. Sanz Castillo, S. Brisigotti, D. Nardelli and M. Tropeano "*Tensile and bending strain tolerance of ex situ MgB2/Ni/Cu Superconductor tape*" IEEE Transaction on applied superconductivity 25 2 1-7 2015